Real and apparent changes in sediment deposition rates through time

Rina Schumer[1] and Douglas J. Jerolmack[2]

Received 15 January 2009; revised 11 May 2009; accepted 2 July 2009; published 30 September 2009.

[1] Field measurements show that estimated sediment deposition rate decreases as a power law function of the measurement interval. This apparent decrease in sediment deposition has been attributed to completeness of the sedimentary record; the effect arises because of incorporation of longer hiatuses in deposition as averaging time is increased. We demonstrate that a heavy-tailed distribution of periods of nondeposition (hiatuses) produces this phenomenon and that observed accumulation rate decreases as $t^{\gamma-1}$, over multiple orders of magnitude, where $0 < \gamma \leq 1$ is the parameter describing the tail of the distribution of quiescent period length. By using continuous time random walks and limit theory, we can estimate the actual average deposition rate from observations of the surface location over time. If geologic and geometric constraints place an upper limit on the length of hiatuses, then average accumulation rates approach a constant value at very long times. Our model suggests an alternative explanation for the apparent increase in global sediment accumulation rates over the last 5 million years.

Citation: Schumer, R., and D. J. Jerolmack (2009), Real and apparent changes in sediment deposition rates through time, *J. Geophys. Res.*, *114*, F00A06, doi:10.1029/2009JF001266.

1. Introduction

[2] Estimating erosion and deposition rates through geologic time is a foundation of geomorphology and sedimentology. Measured rates provide information about the nature and pace of landscape evolution. Modern sediment dating techniques, coupled with biological and chemical proxies for air temperature, precipitation and altitude, promise continued progress in unraveling the coupling of erosion/deposition, tectonics, and climate change. Because sediment transport processes on the Earth's surface respond to glacial cycles and tectonic motions, changes in denudation and accumulation rates through geologic time are expected. Resolving these changes and attributing them to specific forcing mechanisms is a key challenge. For example, much recent research has documented a global increase in sediment accumulation rates since the late Cenozoic ($\sim$5 Ma to present; Figures 1 and 2 [*Zhang et al.*, 2001; *Molnar*, 2004; *Kuhlemann et al.*, 2001]). Those studies present compelling evidence that enhanced climate variability beginning in the late Cenozoic has continually destabilized landscapes and led to enhanced erosion in upland environments.

[3] It is well known that measured deposition rates decrease systemically with measurement duration (Figure 3) for virtually all depositional environments in which there are sufficient data, with intervals ranging from minutes to millions of years [*Sadler*, 1981, 1999]. Here we refer to this pattern as the "Sadler effect." *Sadler* [1981] recognized that this decrease likely results from the intermittent nature of sediment deposition. To better understand this, consider modern sediment accumulation around the globe. If we measure sedimentation everywhere it is occurring, we may estimate a large value for the average global accumulation rate. If we instead consider all basins, including ones experiencing nondeposition or erosion, we would estimate a much smaller value. We can infer that in the temporal evolution of one particular basin, there will be hiatuses in deposition interleaved with intervals of accumulation. Localized, instantaneous rates of deposition (or erosion) are controlled only by the dynamics of sediment transport. Over long timescales, however, deposition rates are limited by the generation of accommodation space, typically the slow process of tectonic subsidence. As an example, consider deposition at a point on a river delta undergoing constant subsidence. Migrating dunes have deposition localized on steep downstream faces, while the longer upstream faces reerode most deposited sediment. In addition, significant sediment transport only occurs during large annual floods, so during most of the year little river sediment deposits at any point on the delta. Following centuries to millennia of channel deposition, a river will avulse to a new location and abandon the old channel. The abandoned section of the delta will flood for millennia because of continued subsidence, until the river eventually returns to begin deposition anew. The result is that hiatuses would dominate the depositional history at any place on the delta, and would have a wide distribution in time, even under steady climate and tectonic conditions. Geologic evidence strongly supports the notion that hiatuses are common while deposition is rare, such that stratigraphy records only a very

[1]Division of Hydrologic Sciences, Desert Research Institute, Reno, Nevada, USA.
[2]Department of Earth and Environmental Science, University of Pennsylvania, Philadelphia, Pennsylvania, USA.

0148-0227/09/2009JF001266

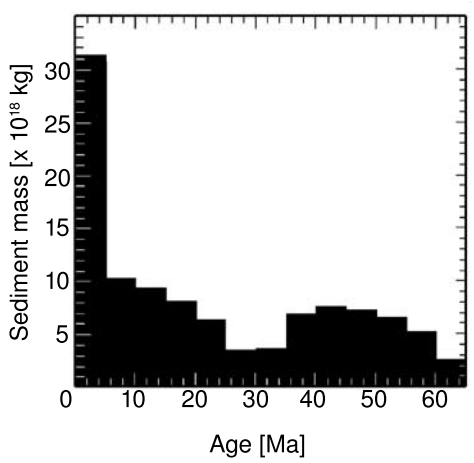

Figure 1. Global values for seafloor sediment accumulation [after *Hay et al.*, 1988; *Molnar*, 2004]. Note that data are separated into bins with an interval of 5 million years. In this context, accumulation during the last 5 million years appears to abruptly increase.

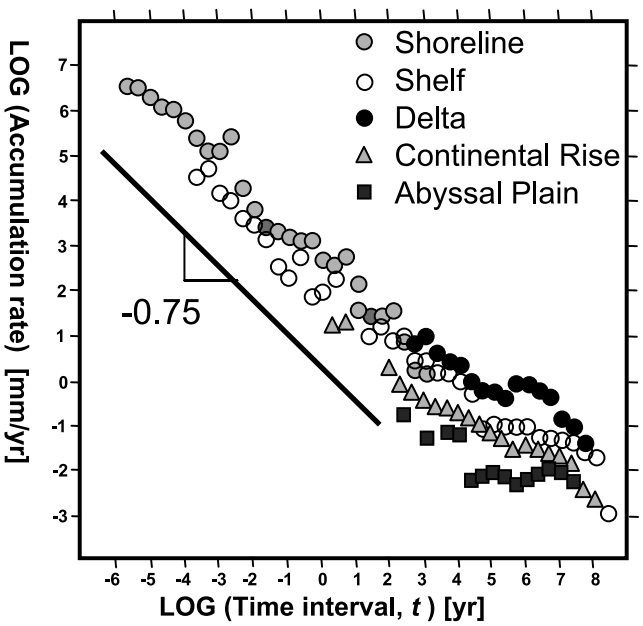

Figure 3. Representative "Sadler plot" showing sediment accumulation rates as a function of measurement interval for siliciclastic shelf deposits. Data are log-bin averaged and represent thousands of measurements for each different environment. At long timescales, some data appear to gradually converge toward a constant rate.

small fraction of Earth surface evolution [*Sadler*, 1981; *Tipper*, 1983]. *Sadler* [1981] hypothesized that the apparent decrease in accumulation rate with increasing measurement interval arises because of incorporation of longer hiatuses in deposition as averaging time is increased.

[4] Observations in natural rivers show that sediment rarely is conveyed steadily downstream, but instead pulses in an unpredictable fashion [*Leopold et al.*, 1964; *Gomez et al.*, 2002]. Careful laboratory experiments with constant boundary conditions have produced large-scale fluctuations in bed load transport rates [*Singh et al.*, 2009] and for shoreline migration in a fan delta [*Kim and Jerolmack*, 2008]. Mechanisms responsible for these fluctuations in fluvial systems include (in increasing length and timescale): the direct influence of turbulence on grain entrainment [*Schmeeckle and Nelson*, 2003; *Sumer et al.*, 2003] and grain-grain interactions in a river bed [*Drake et al.*, 1988]; migration of bed forms [e.g., *Jerolmack and Mohrig*,

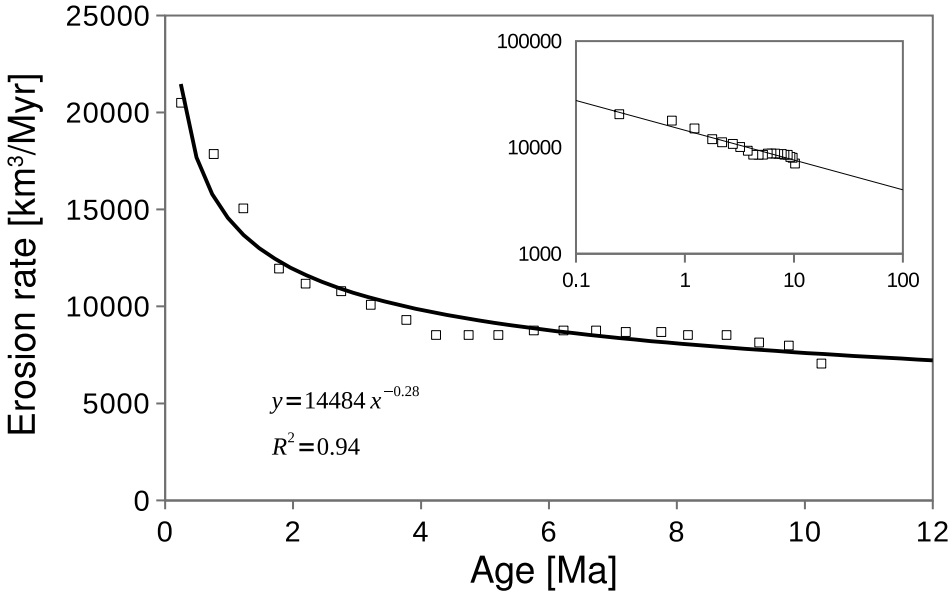

Figure 2. Volumetric erosion rates for the last 10 Myr from the Eastern Alps (data from *Kuhlemann et al.* [2001]). Rates were estimated from measurements of sediment accumulation in basins around the Alps and were corrected for compaction. The curve may be thought of equivalently as sediment accumulation rate. Inset shows data plotted on a log-log scale.

2005a]; river avulsion and channel migration [*Jerolmack and Paola*, 2007]; and large-scale slope fluctuations in a river delta [*Kim and Jerolmack*, 2008]. Nonlinear thresholds exist in many other types of transport systems as well. Regardless of their origin, the net effect of such nonlinearities is that sediment transport is intermittent and rates typically vary widely in space and time even under steady forcing. Several studies indicate that a large portion of stratigraphy may be the record of the stochastic variability of sediment transport itself, rather than changes in forcing [*Sadler and Strauss*, 1990; *Paola and Borgman*, 1991; *Pelletier and Turcotte*, 1997; *Jerolmack and Mohrig*, 2005b; *Jerolmack and Sadler*, 2007; *Kim and Jerolmack*, 2008].

[5] Unequivocal demonstration of real changes in accumulation rate through geologic time, such as the postulated late Cenozoic increase of *Molnar* [2004], requires that these rates are measured over a constant interval of time t [*Gardner et al.*, 1987]. This is rarely possible with real data, however, where modern rates are measured over short time intervals while historical and geological rates are measured over longer and longer intervals [*Sadler*, 1981, 1999]. For example, *Hay et al.* [1988] presented data on mass accumulation of sediment in the world's oceans through time (Figure 1). For their method the "area of seafloor in existence at 5-Myr intervals from 0 to 180 M" was determined, and each area "was multiplied by the average solid phase sediment accumulation rate for the interval" [*Hay et al.*, 1988, p. 14,934]. Estimates for accumulation rates, however, were not from equal time intervals; they came from thousands of nonuniformly spaced dated horizons in dozens of Deep Sea Drilling Project cores. In effect, rates were determined in the same manner (and using some of the same data) as *Sadler* [1981, 1999], but then transformed into uniform intervals for convenience. The data from *Kuhlemann et al.* [2001] share similar issues (Figure 2). *Sadler* [1981] demonstrated that age and time interval cannot be separated from each other in estimates of sediment accumulation; indeed, his data show an almost one-to-one correlation between sample age and measurement interval. The result is that the measurement interval systematically increases with the age of the deposit, and thus real changes in sediment accumulation rates ("process rates" in the work by *Gardner et al.* [1987]) are difficult to separate from apparent changes because of the Sadler effect. Determining the nature of stochastic transport fluctuations, therefore, is of paramount importance, and determining their effect on the geologic record requires modeling.

2. Previous Stochastic Models for Sediment Deposition

[6] The story of depositional history can be told by following the elevation of the sediment surface with time $S(t)$. In this study, we refer to true sediment deposition rate as the velocity V of the sediment surface during deposition. The effective average deposition rate, however, estimated by taking the ratio of accumulation thickness to endpoint dates $V_{\mathrm{obs}} = \frac{S(t_2)-S(t_1)}{t_2-t_1}$, reflects the true deposition rate as well as depositional hiatuses (periods of zero velocity) and erosion (negative surface velocity), with a possible correction for compaction. Modeling the generation of stratigraphy as a stochastic process has a long history beginning with *Kolmogorov* [1951]. The idea is that location of the sediment surface is the sum of past depositional and erosional periods, represented by positive or negative "jumps" creating a stratigraphic column. Given independent and identically distributed (IID) particle jump vectors Y_n, location of the sediment surface at time t is

$$S(t) = \sum_{i=1}^{t/\Delta t} Y_i, \tag{1}$$

where Δt is the time between jumps. As equation (1) implies, the focus of these stochastic models has been on the nature of depositional and erosional periods that affect the location of the sediment surface $S(t)$ in space. These have included exponentially distributed bed thickness [e.g., *Dacey*, 1979] and skewed distributions that produce biased random walks and lead to a negative dependence of V_{obs} on t [*Tipper*, 1983].

[7] Others have used the continuous scaling limit of the classical random walk to represent sediment deposition. For example, a one-dimensional Brownian motion was used to represent a rising (deposition) or declining (erosion) sedimentary surface, while a deterministic drift term represented the generation of accommodation space (e.g., steady tectonic subsidence [*Strauss and Sadler*, 1989]). This model reproduced the general form of empirical scaling curves with two asymptotes: over shorter time intervals, accumulation was determined principally by noise, while long timescales were dominated by the drift term. The short time scaling behavior of accumulation rate for this model follows the form $V_{\mathrm{obs}} \propto t^{-1/2}$, while at long time intervals accumulation rate is constant and equal to drift, thus $V_{\mathrm{obs}} \propto t^{0}$. The diffusion equation has been used to model sediment deposition with distance from a source [*Paola et al.*, 1992]. An additional noise term can account for the random location of the source and other known physical processes [*Pelletier and Turcotte*, 1997]. This model led to $V_{\mathrm{obs}} \propto t^{-3/4}$, in good agreement with empirical data for fluvial systems. The source of this scaling was correlation in depositional increments. Others have added correlation to the spatial increments by using fractional Brownian motion models [*Sadler*, 1999; *Molchan and Turcotte*, 2002; *Huybers and Wunsch*, 2004].

[8] Exceptions to the focus on the spatial process began with *Plotnick* [1986], who showed that a power law relationship between accumulation rate and time interval implies a power law distribution of hiatus periods in deposition. This was demonstrated by creating a synthetic stratigraphic column and removing portions according to the recipe for generating a Cantor set. This model resulted in a unique scaling rate: $V_{\mathrm{obs}} \propto t^{-1/2}$ for the accumulation rate according to the exact scaling of a Cantor set. Other models have been used to generate synthetic sequences with power law hiatus periods. One example is a bounded random walk model (erosion or deposition occurring randomly with net accumulation always positive) also resulting in $V_{\mathrm{obs}} \propto t^{-1/2}$ [*Pelletier*, 2007]. These studies demonstrate the link between heavy tailed quiescent periods and scaling in observed accumulation rate, but their focus is models for

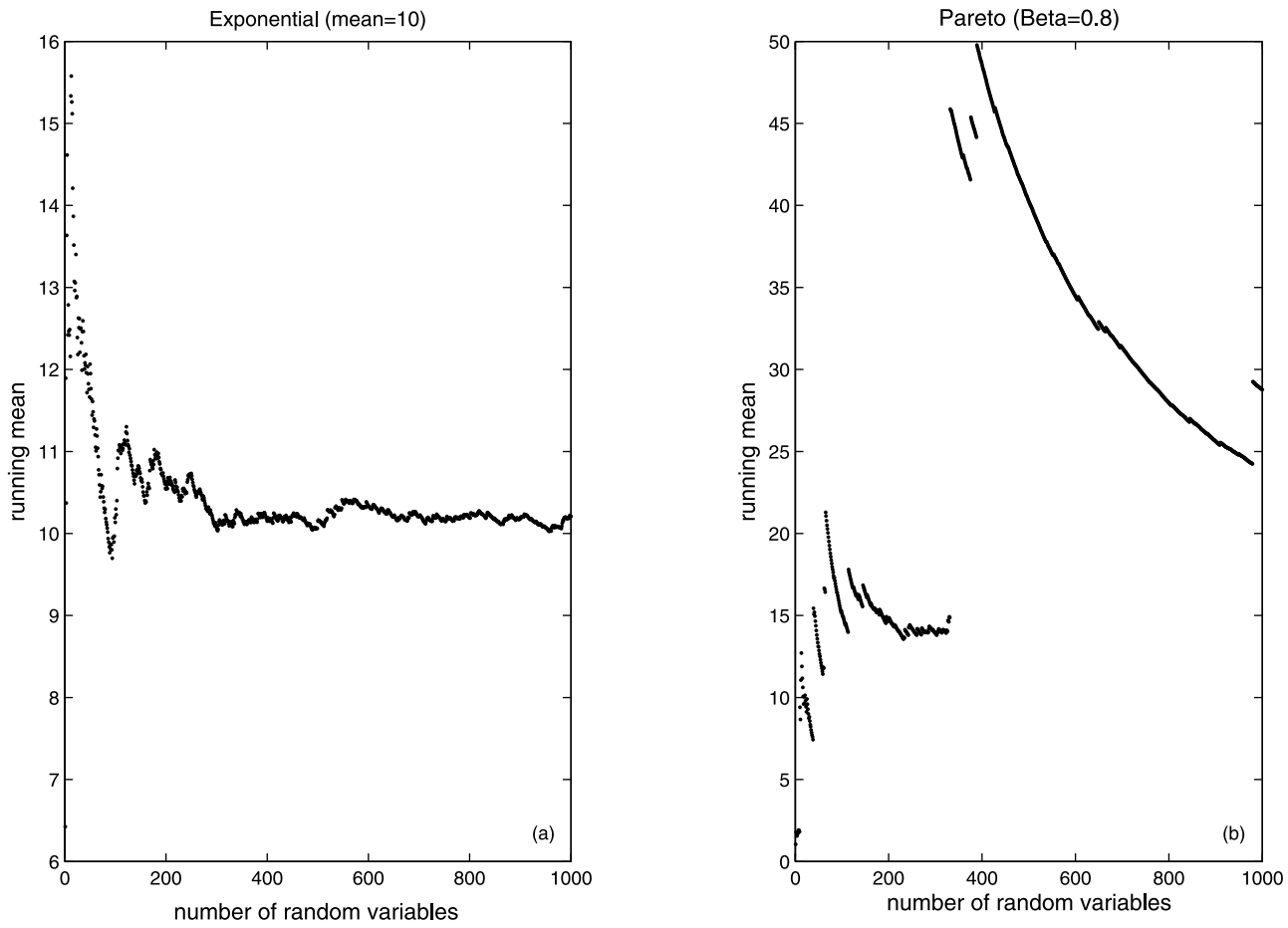

Figure 4. Running average for series of (a) exponential random variables and (b) Pareto random variables. The law of large numbers shows that the sample mean of a large number of random variables with finite-mean probability density will converge to that mean (Figure 4a). This convergence does not occur if a distribution has infinite mean (Figure 4b).

generating synthetic stratigraphic sequences with power law hiatus distribution. Further, these studies produce specific scaling rates rather than allowing for the range of accumulation scaling observed in the field [*Jerolmack and Sadler*, 2007].

[9] In this work we provide analytical theory underlying the results found by *Plotnick* [1986] and *Pelletier* [2007]. We provide a random model that accommodates power law hiatus periods with arbitrary scaling and use previous results in stochastic limit theory to find the exact relationship between hiatus distribution and accumulation rate. Although we do not treat physical processes of sediment deposition and erosion explicitly, the stochastic model can shed light on the nature of these processes and also on the geologic record itself.

3. Conceptual Model

[10] Like many before us [e.g., *Sadler*, 1981; *Tipper*, 1983; *Plotnick*, 1986; *Pelletier*, 2007], we hypothesize that the great length of nondepositional periods relative to depositional periods results in sequence thickness for a given time interval with a wide distribution. This leads to large variation between true deposition rate V during deposition and observed deposition rate V_{obs} which incorporates periods of nondeposition. It is not possible to predict the length of hiatus or depositional periods and so we can treat accumulation thickness, and thus observed velocity, as random variables.

[11] In probability theory, the law of large numbers (LLN) describes the long-term stability of the mean of a sequence of random variables. The running sample mean for a sequence of random variables drawn from a distribution with finite expected mean converges to the true mean of the distribution (Figure 4a) [*Ross*, 1994]. We suggest, however, that average measured deposition rate does not have a finite expected value because even if an extremely long hiatus occurs, there is still a small but finite probability of an even longer hiatus. The practical implication of a random variable having infinite mean probability density is that the sample mean of a sequence of random variables will never converge to a constant value as the number of samples becomes large (Figure 4b). This is because extremely large values occur often enough to radically change the running sample mean. Infinite-mean probability densities are characterized by a cumulative distribution function (CDF) with tail that decays as power law $t^{-\gamma}$, $0 < \gamma \leq 1$. The probability density function (derivative of the CDF) has a tail that decays as $\sim t^{-\gamma-1}$. Then the expected first moment, or mean, of the density diverges $E(t) \equiv \int_{-\infty}^{\infty} tp(t)dt = \infty$, where

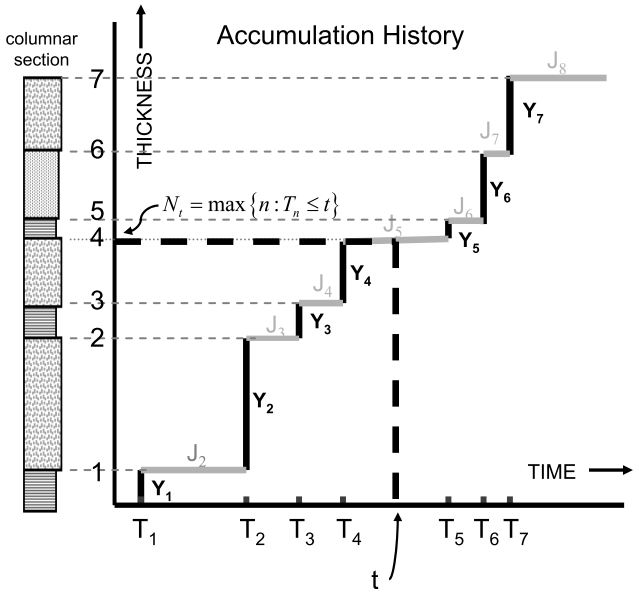

Figure 5. In a CTRW representing the location of the sediment surface with time, permanent accumulation periods are represented by random jumps (Y_i) and hiatuses between permanent accumulation periods are represented by waiting times (J_i). The number of events by time t, T_n, is related to the time of the nth event, N_t (data after *Sadler* [1999] and *Benson et al.* [2007]).

$p()$ represents probability [*Feller*, 1968]. In other words, sample mean of an infinite mean distribution will never converge to a constant value (Figure 4b) because the mean of the parent distribution does not exist.

[12] When the tails of the hiatus duration distribution have infinite mean, an average length hiatus does not emerge. We will show that as the sampling interval increases, so does the probability of encountering an extremely long hiatus, and in turn, the observed deposition rate V_{obs} decreases as a power law.

[13] In most natural sedimentary systems where sufficient data exist, the observed deposition rate appears to approach a constant value at very long time intervals; that is, there is a transition to $\gamma = 1$, and the thickness of sedimentary deposits increases almost linearly with time [*Jerolmack and Sadler*, 2007, Figure 3]. In the infinite-mean waiting time model there is always a finite possibility of a longer hiatus period. In nature, however, there are typically limits to the waiting times and magnitudes of deposition events. Subsidence, the main mechanism for generating accommodation space on geologic timescales, depends on such processes as thermal cooling, sedimentary loading, and deformation, all of which are likely to change through time. Sedimentary basins have a finite lifetime over which subsidence can persist before they are uplifted or subducted by tectonic processes. Finally, there is some limit to the range of climate fluctuations that have occurred in Earth's history, and a maximum timescale associated with that limit. If climate variability drives part of the stochastic variation in deposition rates, this places a limit on the distribution of waiting times between depositional periods. In short, the range of variability in sedimentation rates and timescales determines the range over which the Sadler effect is observed.

4. Theory

[14] The model we use to predict location of the sediment surface with time $S(t)$ is an uncoupled continuous time random walk (CTRW) (see *Metzler and Klafter* [2000] for a comprehensive review), also known as a renewal reward process. A CTRW is a discrete stochastic process (despite its name) that equates location at time t with the sum of discrete jumps (deposition periods) that require a random time to complete because of "waiting times " (hiatuses) between jumps. In uncoupled, as opposed to coupled, CTRW, jumps are not correlated with waiting times.

[15] Conceptually, an infinite average duration between periods of deposition can be interpreted as a succession of long pauses followed by bursts of events [*Balescu*, 1995; *Montroll and Schlesinger*, 1984]. We use a CTRW where constant depositional periods are effectively instantaneous. From a modeling perspective, this simplifies computations and also results in the same long-time result as a model with finite depositional period duration [*Zhang et al.*, 2008]. We judge that limiting, or asymptotic, models are appropriate for representing random processes recorded over geologic time.

[16] Given constant jump vectors Y_n with density $f(x)$, the location of the sediment surface at time t is (Figure 5)

$$S_{N_t} = \sum_{i=1}^{N_t} Y_i, \tag{2}$$

where the number of jumps by time t, N_t, is a function of the random IID waiting times between the initiation of jumps J_i: the time of the nth jump is $T(n) = J_1 + .. + J_n$ and $N(t) = \max\{n{:}T(n) \le t\}$. The density of waiting times J_i is denoted $\psi(t)$. In a detailed model for sediment deposition, deposition rate and durations of depositional periods can be a random variable by assigning a "jump length density". The purpose of our study, however, is to demonstrate the effect of various waiting time distributions, and so we set sediment surface jump lengths Y_n = constant.

[17] The solution to a CTRW is typically given by its Fourier-Laplace transform ($x \to k$, $t \to s$) [*Montroll and Weiss*, 1965; *Scher and Lax*, 1973]. The probability of surface location

$$S(k,s) = \frac{1-\psi(s)}{s}\,\frac{S(k,t=0)}{1-f(k)\psi(s)} \tag{3}$$

is a function of the start location of the surface $S(x, t = 0)$, the jump length density, and the waiting time density. To compare the effects of finite-mean and infinite-mean hiatus length densities we will apply each, in turn, in the CTRW master equation, take the scaling limit to obtain the long-term governing equation, and evaluate the deposition rate characteristics predicted by each. Results in the section describing finite-mean hiatus density are well known. We derive them in detail so that the method used to generalize to the infinite-mean case is clear.

4.1. Finite-Mean Hiatus Duration

[18] Using the infinite series representation of the exponential function, the Laplace transform of the waiting time density $\psi(t)$ can be expressed as

$$\begin{aligned}\psi(s) &= \int e^{-st}\psi(t)dt \\ &= \int (1 - st - ..)\psi(t)dt \\ &= \int \psi(t)dt - s\int t\psi(t)dt - .. \\ &= 1 - s\mu - .. \text{ as } s \to 0. \end{aligned} \quad (4)$$

Since we assume a constant deposition rate, the jump length density will be a dirac delta function at V: $p(x) = \delta(x + C)\Delta t$. Since this function is a probability density with mean C and variance zero, using arguments similar to those in equation (4), its Fourier transform is $f(k) = 1 - ikC$. Let Δt be a characteristic jump time, and rescale the moments of the densities by letting $\beta = \frac{\mu}{\Delta t}$ and $V = \frac{C}{\Delta t}$. Then

$$\begin{aligned} f(k)\psi(s) &= (1 - \beta\Delta ts + O\Delta t)(1 - ikV\Delta t) \\ &= 1 - ikV\Delta t - \beta\Delta ts + ikVs\beta(\Delta t)^2 + O(\Delta t), \end{aligned} \quad (5)$$

where $O(\cdot)$ represent higher-order terms. Use (4) and (5) in the master equation (3), simplify, and take the limit as $\Delta t \to 0$ to find

$$S(k,s) = \frac{s}{s}\frac{\beta S(k,0)}{\beta s + Vik}. \quad (6)$$

[19] Rearrange and take inverse transforms to find that the partial differential equation (PDE) that governs this CTRW with finite-mean waiting time distribution in the scaling limit is an advection equation with retardation coefficient β related to the mean of the waiting time distribution:

$$\beta\frac{\partial S}{\partial t} = -V\frac{\partial S}{\partial x} \quad (7)$$

or

$$\frac{\partial S}{\partial t} = -V_{\text{eff}}\frac{\partial S}{\partial x}. \quad (8)$$

[20] For clarity, V is the actual deposition rate during deposition. The average deposition rate over many deposition/nondepositional periods $V_{\text{eff}} = V/\beta$ incorporates the periods of zero deposition into the estimate of deposition rate. The measured or observed deposition rate V_{obs} is often not equal to, but related to V or V_{eff}. Our goal is to clarify this relationship. Equation (8) has the well known Green's function solution $S(x, t) = \delta(V_{\text{eff}}t)$, a constant shift with time according to the retarded velocity. In other words, after a sufficient time has passed, the location of the sediment surface S grows linearly with time as $E(t) = \frac{Vt}{\beta}$. The expected deposition rate after long time is simply $V_{\text{obs}} = \frac{E(t)}{t} = \frac{V}{\beta}$, a constant. For finite-mean hiatus density, the deposition rate is expected to converge to a constant rate.

4.2. Heavy-Tailed, Infinite-Mean Hiatus Duration

[21] For a CTRW with effectively instantaneous jumps of constant length and infinite-mean waiting time density with tail parameter γ, we have [*Klafter and Silbey*, 1980]

$$\psi(s) = 1 - B^\gamma s^\gamma + .. \quad (9)$$

Rescale the moments of the waiting time density by $\beta = \frac{B^\gamma}{\Delta t}$ and find

$$\begin{aligned} f(k)\psi(s) &= (1 - \beta\Delta ts^\gamma + O\Delta t)(1 - ikV\Delta t) \\ &= 1 - ikV\Delta t - \beta\Delta ts^\gamma + ikVs^\gamma\beta(\Delta t)^2 + O(\Delta t). \end{aligned} \quad (10)$$

[22] Use (9) and (10) in the CTRW master equation (3), simplify and take the limit as $\Delta t \to 0$ to find

$$S(k,s) = \frac{s^{\gamma-1}\beta S(k,0)}{\beta s^\gamma + Vik}. \quad (11)$$

[23] After rearranging and taking inverse transforms, we find that in the scaling limit, the PDE governing a CTRW with constant jump length and infinite mean waiting time distribution is a fractional-in-time advection equation:

$$\beta\frac{\partial^\gamma S}{\partial t^\gamma} = -V\frac{\partial S}{\partial x} \quad (12)$$

or

$$\frac{\partial^\gamma S}{\partial t^\gamma} = -V_{\text{eff}}\frac{\partial S}{\partial x}, \quad (13)$$

where $0 < \gamma \leq 1$ is the order of the fractional time derivative. Background on some useful fractional PDES is provided by *Schumer et al.* [2009] and many others [e.g., *Benson et al.*, 2000; *Schumer et al.*, 2001, 2003; *Meerschaert et al.*, 2002]. Methods to solve fractional-in-time equations of this type can be found in the work by *Baeumer and Meerschaert* [2001]. For the purposes of this study it is sufficient to understand that the noninteger order derivative in equation (12) arises as a result of an infinite mean waiting time density and, as we will show, that the mean of the solution scales as t^γ. This generalizes the integer order case, where $\gamma = 1$ and the expected location of the surface scales as t^1.

[24] To determine the expected location of the surface with time following the fractional advection equation, take Fourier and Laplace transforms, assuming a pulse initial condition and solve for S(k,s):

$$S(k,s) = \frac{s^{\gamma-1}}{s^\gamma + \frac{V}{\beta}ik}. \quad (14)$$

Since the solution $S(x, t)$ of (12) is a probability density, its first moment or expected location with time, can be calculated using [e.g., *Ross*, 1994]

$$E(S) = \frac{1}{-i}\frac{\partial S(k,s)}{\partial k}|_{k=0}. \quad (15)$$

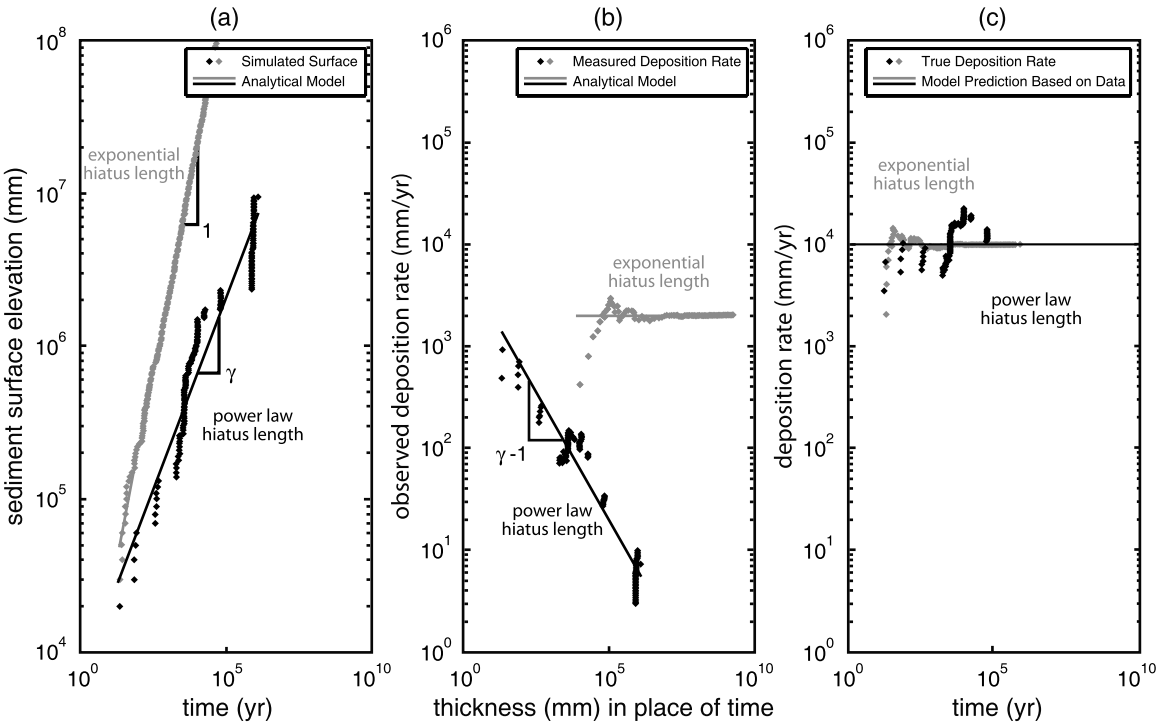

Figure 6. Comparison of simulations of constant rate (10^4 mm/year) sediment deposition periods that last 1 year where random quiescent periods are drawn either from an exponential distribution (gray) with average length $\frac{1}{\lambda} = \frac{1}{5}$ years or from a Pareto distribution (black) with tail parameter $\gamma = 0.5$. (a) Graph of simulated sediment surface location with time, (b) Sadler-type graph of estimated deposition rate versus thickness of unit measured, and (c) theoretical estimate of the actual velocity based on each observation in Figure 6b.

Substituting (14) in (15) and taking the inverse Laplace transform, we find

$$E(S) = \frac{V}{\beta}\frac{t^{\gamma}}{\Gamma(1+\gamma)}, \tag{16}$$

where $\Gamma(\cdot)$ is the Gamma function. The measured velocity $V_{\mathrm{obs}}(t) = \frac{E(S)}{t}$ will be

$$V_{\mathrm{obs}}(t) = \frac{V}{\beta}\frac{t^{\gamma-1}}{\Gamma(1+\gamma)}, \tag{17}$$

where t represents the time interval through which deposition rate is measured. This equation describing measured deposition rates (equation (17)) demonstrates that measured sediment deposition with heavy-tailed quiescent periods has power law decay with log-log slope $\gamma - 1$. In other words, our analysis shows formally how a power law distribution of hiatuses can produce the Sadler effect. If there is no mean quiescent period, there is no mean effective velocity, and we never converge to any effective velocity as we sample larger and larger sedimentary sequences that include extreme quiescent periods.

4.3. Truncated Infinite-Mean Hiatus Duration

[25] There have been a variety of applications for which a model with infinitely large waiting times is unacceptable, leading to the replacement of an infinite-mean waiting time density with a truncated or tempered version [*Hui-fang*, 1988; *Dentz et al.*, 2004; *Meerschaert et al.*, 2008]. Tempered densities have power law character for small time and exponential character above some cutoff. These densities have finite moments so that the solutions of governing equations for CTRW that use them have a converging mean. CTRW with tempered waiting time density are appropriate for cases in which the observed accumulation rate decreases as a power law and then converges to an approximately constant rate. Tempered advection-dispersion equations governing these CTRW are described by *Meerschaert et al.* [2008]. The nature of the intermediate character and late time convergence of accumulation rate graphs will be examined in future work. For this study, the power law portion of the accumulation rate graph will be used to estimate true deposition rate.

5. Simulation

[26] To demonstrate the effect of power law versus thin-tailed hiatus length distribution resulting in time-dependent observed deposition rate, we simulated a variety of discrete CTRWs. For each, we alternately sampled a hiatus period length from the appropriate probability density and then added a constant deposition thickness to the simulated stratigraphic column (Figure 6a). Deposition rate for each simulation was calculated after each deposition period using $V_{\mathrm{obs}_i} = \frac{S(t_i)-S(t_0)}{t_i-t_0}$ (Figure 6b).

5.1. Finite-Mean Hiatus Duration

[27] Finite-mean waiting time CTRWs were simulated using exponential hiatus lengths $\psi(t) = \lambda e^{-\lambda t}$, with rate $\lambda = 5$. Constant depositional periods were 1 year long with velocity 10^4 mm/year. The mean of an exponential distribution is $\mu = \frac{1}{\lambda}$ so the effective deposition rate is the actual deposition rate divided (retarded) by the length of the average quiescent time (if the surface only increases 1 year in each deposition period): $V_{\text{eff}} = V\lambda$ As predicted, the elevation of the simulated sediment surface increased linearly with time as $S(t) = V\lambda t = 10^4 = \frac{1}{5}t$ (Figure 6a). Since average hiatus length exists in this case, estimates of effective deposition rate quickly converge to V_{eff}, the average deposition rate divided by the average hiatus length (Figure 6b). This phenomena is the same as that described in Figure 4a. Knowledge of the average duration of hiatuses between depositional periods is required to estimate actual deposition rate from the observed rate V_{eff} (Figure 6c).

5.2. Infinite-Mean Hiatus Duration

[28] We simulated infinite-mean waiting time CTRW using Pareto distributed hiatus lengths $\psi(t) = \gamma\, t^{-\gamma-1}$ with tail parameter $\gamma = 0.5$ and tracked sediment surface location through time. As in the previous case, we used constant depositional periods 1 year long with velocity 10^4 mm/year. For the case of Pareto waiting times, the retardation coefficient is $\beta = \Gamma(1-\gamma)$ (Appendix A), yielding an expected sediment surface elevation with time

$$E(S) = \frac{V}{\Gamma(1-\gamma)}\frac{t^{\gamma}}{\Gamma(1+\gamma)}. \tag{18}$$

Using $V_{\text{obs}} = \frac{E(S)}{t}$, we find

$$V_{\text{obs}}(t) = \frac{V}{\Gamma(1-\gamma)}\frac{t^{\gamma-1}}{\Gamma(1+\gamma)}. \tag{19}$$

We see rapid convergence of the sediment surface location and observed deposition rates to these equations in Figures 6a and 6b.

[29] True average deposition rate can be estimated from observations by following the line in the graph (Figure 6b) toward zero or rearranging equation (18): $V = \frac{V_{\text{obs}}\Gamma(1-\gamma)\Gamma(1+\gamma)}{t^{\gamma-1}}$. The value for the waiting time tail distribution γ can be obtained by measuring the slope of observed velocity versus time graph (Figure 6b). Because of the random nature of the data, the value will not be exact. In this simulation, the true deposition rate estimated from the observed deposition rates with time fluctuated over 1 order of magnitude approximately centered at the true deposition rate.

5.3. Heavy-Tailed Hiatus Duration With Finite Maximum

[30] We generated discrete CTRW with exponentially tempered Pareto waiting time distribution ($\gamma = 0.4$, $\lambda = 10{,}000$), constant depositional periods 1 year long, and velocity 10^4 mm/year. We generated tempered Pareto random variables using the method described by B. Baeumer and M. Meerschaert (Tempered stable Lévy motion and transient super-diffusion, submitted manuscript, 2009). At early time, the simulated surface appears to follow the infinite mean model, with log-log slope γ (Figure 7a). After a cutoff time, the slope becomes linear. This change in slope coincides with convergence of the observed accumulation rate (Figure 7b).

6. Application

[31] A heavier tail in the hiatus density (smaller γ) results in larger probabilities of extremely long quiescent periods. To evaluate different environments, we return to data reported in Table 1 of *Jerolmack and Sadler* [2007] on terrigenous shelf deposits; these include continental rise and slope, continental shelf, shore, delta, floodplain, and alluvial channel deposits. For time intervals smaller than 10^2 yr, all environments for which sufficient data exist show $\gamma < 0.50$, indicating significant probabilities of long hiatuses. The smallest value was for alluvial channel deposits ($\gamma = 0.17$). Such deposits are constructed mostly by the process of channel avulsion, an abrupt change in channel path induced by deposition. Recent modeling work has suggested that avulsion is a nonlinear threshold process, which produces heavy-tailed dynamics in both channel migration and sediment deposition [*Jerolmack and Paola*, 2007], consistent with a heavy tail in hiatus density. The environment with the largest value ($\gamma = 0.48$) of those listed is river floodplains. Floodplain sedimentation is most rapid in the vicinity of channels, but deposition on floodplains persists even at significant distances from active rivers. Data suggest that floodplains have a lower probability of long hiatuses in deposition than do channel deposits.

[32] We now turn our attention to implications of this work for interpreting real changes in mean accumulation rates through geologic time. Measured sedimentation rates in basins (and, by inference, erosion of uplands) around the world show a 2–10 fold increase in the last 5 Myr when compared to previous time intervals [*Hay et al.*, 1988; *Zhang et al.*, 2001] (Figures 1 and 2). We return to Figure 1, which shows global accumulation of terrigenous sediment in ocean basins, grouped into bins of 5-million-year intervals. It is clear that the mass of sediment accumulated in the last 5 million years is substantially larger than any previous interval. The higher-resolution data from the Eastern Alps [*Kuhlemann et al.*, 2001] (Figure 2) show a similar trend in that erosion rates (or equivalently accumulation rates) appear to diminish with time into the past.

[33] Various explanations for the increase of erosion rates since the late Cenozoic have been proposed [*Zhang et al.*, 2001; *Molnar*, 2004]: the lowering of sea level and subsequent erosion of continental margins; increased glacial erosion and sediment production from a cooler climate; and rapid tectonic uplift. The synchroneity of accelerated accumulation in basins of different geologic context, however, led Molnar and colleagues to dismiss these explanations. They proposed that enhanced climate variability beginning in the late Cenozoic has continually destabilized landscapes and led to enhanced erosion in upland environments. They present compelling evidence of both climatic variation, and a general cooling trend, during the last 5 million years: oxygen isotope records, fossil assemblages, paleosols, and sediment grain size data. Our analysis, however, leads us to question whether the apparent change in accumulation rates can be attributed completely to real

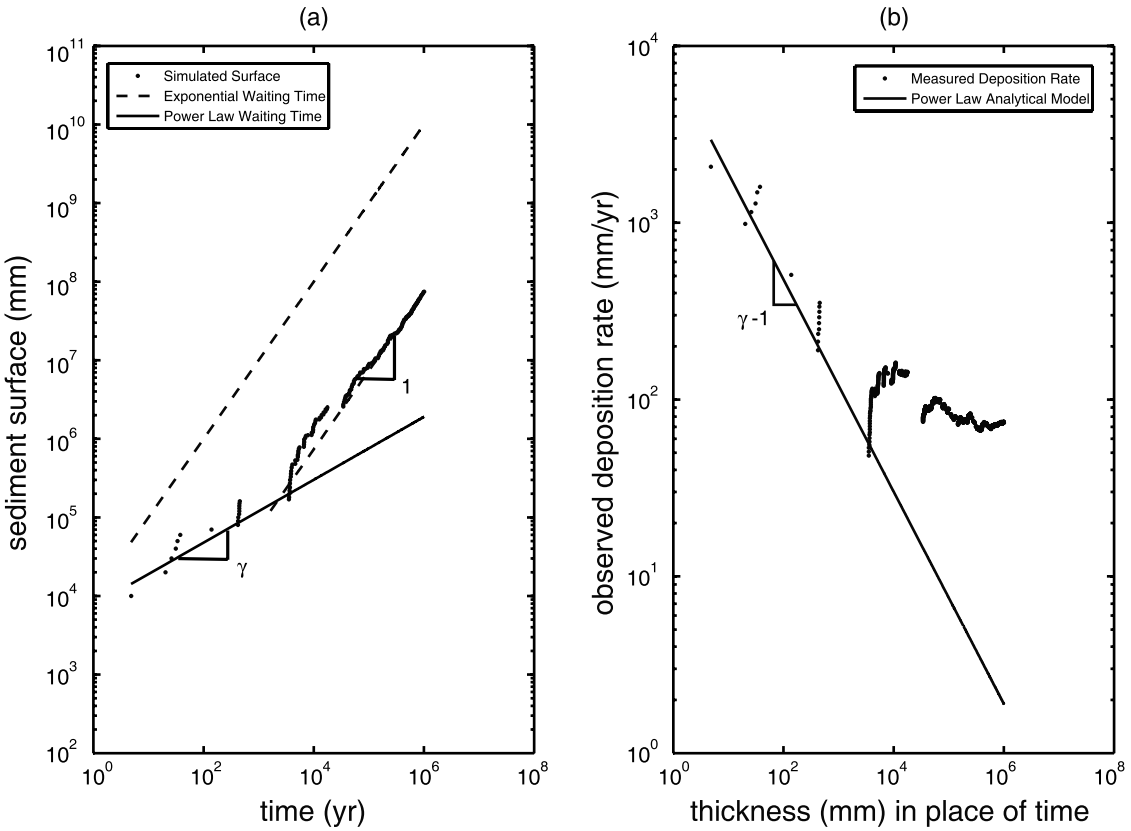

Figure 7. (a) The simulated surface for a CTRW with tempered Pareto ($\gamma = 0.4$, $\lambda = 1/10{,}000$) waiting time distribution begins close to that of the nontruncated Pareto model with equal tail parameter but then converges to the slope of a finite-mean model. (b) Observed deposition rate for this simulation decays as the infinite mean model predicts and then converges to a constant value.

changes in landscape denudation. As discussed previously, we cannot separate sediment age from the interval associated with that measurement. As one test, we present a null hypothesis model for comparison with the sedimentary data just discussed. Figure 8 shows a Sadler-type plot of accumulation rate against time interval for data taken from carbonate platforms. We choose carbonate data because (1) growth rates of carbonate platforms should not be directly related to continental denudation rates and (2) if it is true that climate has generally cooled in the last 5 million years, then real rates of carbonate accumulation should be slower in recent times than in the past (carbonate deposition rate increases with water temperature) and thus rates of carbonate accumulation might be expected to increase with measurement interval (e.g., present to 2 million years ago versus present to 5 million years ago). Just as in every other environment, however, carbonate accumulation rates decrease as a power law function of measurement interval. The data decay at a rate of $t^{-0.39}$, suggesting a hiatus density tail parameter $\gamma = 0.61$ and a true average deposition rate of 50–70 mm/yr.

[34] For a more direct comparison to rate data from the Eastern Alps, we plot carbonate data through a similar time interval in Figure 8 (bottom). The data are very well fit by a power law, and in fact the scaling exponent ($t^{-0.23}$) is very close to that observed for accumulation rates in the Eastern Alps ($t^{-0.28}$). In other words, the change in the apparent rate of carbonate accumulation with measurement interval (Figure 8, bottom) is very similar to the purported real change in mountain denudation rates with age (Figure 2). Observed Eastern Alps denudation rate decreases as a power law function of age like $V_{obs} \sim t^{-0.28}$, meaning $\gamma = 0.72$. While observed rates range between ~2000 and 20,000 km^3/Myr, we estimate (using equation (18)) that the true average denudation rate is approximately 40,000 km^3/Myr. This estimate assumes that hiatus periods far outweigh erosional periods in creating the sedimentary record. Although one cannot prove that the Sadler effect accounts for all of the measured change in accumulation rates of the late Cenozoic, it is equally problematic to assert that measurements reflect real changes in the pace of geologic processes.

7. Discussion

[35] We have described the character of sediment accumulation resulting from a heavy-tailed distribution of waiting times between events. Estimates of deposition rate for specific studies may require inclusion of the stochastic nature of deposition and erosion. Here, we discuss the means by which they can be incorporated into a CTRW model and the impact it will have on model prediction.

[36] 1. Random, thin-tailed depositional period length or rate will not affect the average deposition rate over geologic timescales. CTRW jumps Y_i can be random variables from a parent distribution with both positive (deposition) or negative (erosion) values. In the scaling limit, a CTRW with

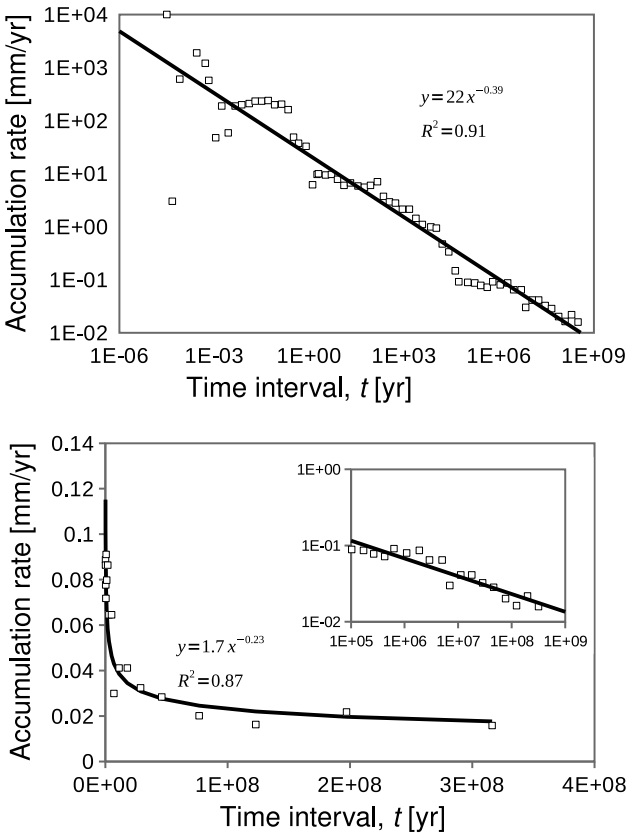

Figure 8. Rates of carbonate platform accumulation plotted against measurement interval, from *Sadler* [1999]. Data are log-bin averaged on the basis of more than 15,000 rate measurements from peritidal settings all over the world. (top) The entire range of data shows carbonate accumulation rates decrease with time as $t^{-0.39}$. (bottom) A subset of the data showing measurements made over intervals comparable to that of the Eastern Alps data shown in Figure 2. Over this range, accumulation rates decrease as $t^{-0.23}$, comparable to the Eastern Alps data. Inset shows data on a log-log scale.

random thin-tailed depositional periods will converge to the same limit process as the CTRW with constant depositional rate with an extra term representing deviation around the mean [*Meerschaert and Scheffler*, 2004]. The governing equation in this case is a fractional-in-time advection-dispersion equation

$$\frac{\partial^\gamma S}{\partial t^\gamma} = -V\frac{\partial S}{\partial x} + D\frac{\partial^2 S}{\partial x^2}, \tag{20}$$

where D is the dispersion coefficient describing spread around the average accumulation rate V. The average sedimentation rate is affected by the order of the temporal derivative (γ) and the order of the derivative in the sediment velocity term (unity): average location of the sediment surface grows as $(Vt)^{\gamma/1}$ [*Zhang et al.*, 2008].

[37] 2. Random, heavy-tailed depositional period length or rate can lead to an increase in measured deposition rates with measurement interval. Here, longer measurement interval leads to increased probability of encountering a depositional period that left an extremely thick sedimentary sequence. Heavy-tailed (infinite-variance) rates of deposition in a CTRW lead, in the scaling limit, to a governing equation with a fractional derivative in the dispersive term: $\frac{\partial^\gamma S}{\partial t^\gamma} = -V\frac{\partial S}{\partial x} + D\frac{\partial^\alpha S}{\partial x^\alpha}$, $1 < \alpha \leq 2$ affecting only the scaling of dispersion in the location of the sediment surface [*Benson et al.*, 2000]. In other words, the scaling of the average velocity will not be affected by deposition rates with heavy-tailed, infinite variance distributions. If deposition rates could be so extreme that their mean value did not converge, then longer measurement interval would be more likely to intersect extremely high deposition rates, and observed accumulation rate would increase with measurement interval. This phenomenon has been observed in mountain erosion rates [*Kirchner et al.*, 2001].

8. Conclusions

[38] We have demonstrated that a heavy-tailed distribution of hiatus periods will result in a power law decrease in observed deposition rate as the measurement interval increases, according to $t^{\gamma-1}$, where γ is the tail parameter of the hiatus density. A more detailed picture of sediment deposition can easily be incorporated into this model.

[39] The best model fit to empirical scaling curves is the truncated Pareto distribution for hiatus periods. This model implies that there is a power law distribution of waiting times between deposition events, but there is an upper limit to this distribution. Geologic and geometric constraints determine this upper limit, beyond which accumulation rates are (nearly) independent of time.

[40] There is ample evidence that sediment transport is a stochastic process even under steady forcing, and that this variability leaves its imprint on the stratigraphic record. We have modeled sediment deposition as an intermittent, heavy-tailed process without describing the source of that intermittency. It seems likely that a large part of the intermittency results from nonlinear dynamics of sediment transport itself, with variability in forcing an additional component. While our stochastic model does not incorporate physical processes, hiatus density distributions inferred from empirical data can provide information of the statistical nature of sediment deposition on geologic timescales. This information would allow comparison of depositional dynamics among different environments, and provide constraints for future process-based models. Further, by fitting the model to empirical scaling curves we can estimate a representative, real value for ''average'' accumulation rates.

[41] Our analysis highlights the difficulty in attributing observed changes in accumulation rates through time to real changes in the rates of erosion and deposition. In particular, we have questioned how much of the observed increase in accumulation rates since the late Cenozoic has to do with accelerated continental denudation due to climate change. There is overwhelming empirical evidence for variability in deposition rate, and it is a mathematical inevitability that such stochastic fluctuations produce a time dependence in accumulation rate measurements. It therefore seems likely that the primary signal in stratigraphy is the record of the

nonlinear dynamics of sediment transport, played out through geologic time.

Appendix A: Approximation of the Retardation Coefficient for a Fractional-in-Time Transport Equation With Pareto Waiting Times

[42] The fractional in time equation $\beta\frac{\partial^\gamma C}{\partial t^\gamma} = L(x)C$, where $L(x)$ is a linear operator, governs the scaling limit of a CTRW with waiting time density $\psi(s) = 1 - \beta s^\gamma + .., 0 < \gamma < 1$ as $s \rightarrow 0$. Here we solve for β given Pareto waiting time density $\psi(t) = \gamma\, t^{-\gamma-1}$.

[43] Use the Laplace transform pair [*Balescu*, 1995]:

$$\psi(s) = 1 - \tau_D^\gamma s^\gamma + .., 0 < \gamma < 1 \,\text{as}\, s \rightarrow 0$$

$$\psi(t) = \frac{1}{\tau_D}\frac{\gamma}{\Gamma(1-\gamma)}\left[\frac{t}{\tau_D}\right]^{-1-\gamma} + .. \,\text{as}\, t \rightarrow \infty,$$

where τ_D is a characteristic time for a CTRW.

[44] Ignore higher-order terms and rearrange to find

$$\psi(t) = \frac{1}{\tau_D}\left(\frac{1}{\tau_D}\right)^{-1-\gamma}\frac{1}{\Gamma(1-\gamma)}\gamma t^{-1-\gamma} = \left(\frac{1}{\tau_D}\right)^{-\gamma}\frac{1}{\Gamma(1-\gamma)}\gamma t^{-1-\gamma}. \quad \text{(A1)}$$

[45] Let $\beta = \tau_D^\gamma$ and use $\tau_D = \beta^{1/\gamma}$ in $\psi(t)$:

$$\psi(t) = \left(\frac{1}{\beta^{-\gamma}}\right)^{1/\gamma}\frac{1}{\Gamma(1-\gamma)}\gamma t^{-1-\gamma} = \beta\frac{1}{\Gamma(1-\gamma)}\gamma t^{-1-\gamma}. \quad \text{(A2)}$$

[46] For the case $\psi(t) = \gamma\, t^{-\gamma-1}$, it must be true that $\beta = \Gamma(1-\gamma)$ with a characteristic time $\tau_D = [\Gamma(1-\gamma)]^{1/\gamma}$.

Notation

- α order of fractional space derivative
- β ratio of true deposition rate and effective deposition rate
- $\delta(x)$ dirac delta function
- γ order of fractional time derivative
- $\Gamma()$ Gamma function
- λ exponential rate parameter
- $\psi(t)$ CTRW hiatus length density
- $\psi(s)$ Laplace transform of CTRW hiatus length density
- D dispersion coefficient
- $f(x)$ CTRW jump length density
- $f(k)$ Fourier transform of CTRW jump length density
- J_i CTRW random hiatus length
- $N(t)$ number of depositional periods by time t
- $S(t)$ location of sediment surface with time
- t time
- V true deposition rate (surface velocity) during deposition
- V_{eff} average deposition rate includes the effect of both deposition and hiatuses
- V_{obs} measured deposition rate
- x distance along the stratigraphic column
- Y_i CTRW random jump length

[47] **Acknowledgments.** We gratefully acknowledge Pete Sadler for providing data for Figure 3 and for continued inspiration on this topic. NCED, an NSF Science and Technology Center at the University of Minnesota funded under agreement EAR-0120914, and the Water Cycle Dynamics in a Changing Environment hydrologic synthesis project (University of Illinois, funded under agreement EAR-0636043) cosponsored the STRESS working group meeting (Lake Tahoe, November 2007) that fostered the research presented here. Insightful comments by three reviewers and the editor improved early versions of this manuscript. Thank you also to Greg Pohll, Mark Meerschaert, and John Warwick for fruitful discussions. R.S. was partially supported by NSF grant EPS-0447416.

References

Baeumer, B., and M. M. Meerschaert (2001), Stochastic solutions for fractional Cauchy problems, *Fract. Calculus Appl. Anal.*, *4*(4), 481–500.

Balescu, R. (1995), Anomalous transport in turbulent plasmas and continuous time random walks, *Phys. Rev. E*, *51*(5), 4807–4822.

Benson, D. A., S. W. Wheatcraft, and M. M. Meerschaert (2000), The fractional-order governing equation of Lévy motion, *Water Resour. Res.*, *36*(6), 1413–1423.

Benson, D. A., R. Schumer, and M. M. Meerschaert (2007), Recurrence of extreme events with power-law interarrival times, *Geophys. Res. Lett.*, *34*, L16404, doi:10.1029/2007GL030767.

Dacey, M. F. (1979), Models of bed formation, *J. Int. Assoc. Math. Geol.*, *11*(6), 655–668.

Dentz, M., A. Cortis, H. Scher, and B. Berkowitz (2004), Time behavior of solute transport in heterogeneous media: Transition from anomalous to normal transport, *Adv. Water Resour.*, *27*(2), 155–173.

Drake, T. G., R. L. Shreve, W. E. Dietrich, P. J. Whiting, and L. B. Leopold (1988), Bedload transport of fine gravel observed by motion-picture photography, *J. Fluid Mech.*, *192*, 193–217.

Feller, W. (1968), *An Introduction to Probability Theory and Its Applications*, vol. 1, John Wiley, New York.

Gardner, T. W., D. W. Jorgensen, C. Shuman, and C. R. Lemieux (1987), Geomorphic and tectonic process rates: Effects of measured time interval, *Geology*, *15*, 259–261.

Gomez, B., M. Page, P. Bak, and N. Trustrum (2002), Self-organized criticality in layered, lacustrine sediments formed by landsliding, *Geology*, *30*, 519–522.

Hay, W. W., J. L. Sloan, and C. N. Wold (1988), Mass/age distribution and composition of sediments on the ocean floor and the global rate of sediment subduction, *J. Geophys. Res.*, *93*(B12), 14,933–14,940.

Hui-fang, D. (1988), Asymptotic behaviors of the waiting-time distribution function $\psi(t)$ and asymptotic solutions of continuous-time random-walk problems, *Phys. Rev. B*, *37*(4), 2212–2219.

Huybers, P., and C. Wunsch (2004), A depth-derived Pleistocene age model: Uncertainty estimates, sedimentation variability, and nonlinear climate change, *Paleoceanography*, *19*, PA1028, doi:10.1029/2002PA000857.

Jerolmack, D., and D. Mohrig (2005a), Interactions between bed forms: Topography, turbulence, and transport, *J. Geophys. Res.*, *110*, F02014, doi:10.1029/2004JF000126.

Jerolmack, D. J., and D. Mohrig (2005b), Frozen dynamics of migrating bedforms, *Geology*, *33*, 57–60.

Jerolmack, D. J., and C. Paola (2007), Complexity in a cellular model of river avulsion, *Geomorphology*, *91*(3–4), 259–270.

Jerolmack, D. J., and P. Sadler (2007), Transience and persistence in the depositional record of continental margins, *J. Geophys. Res.*, *112*, F03S13, doi:10.1029/2006JF000555.

Kim, W., and D. J. Jerolmack (2008), The pulse of calm fan deltas, *J. Geol.*, *116*(4), 315–330.

Kirchner, J. W., R. C. Finkel, C. S. Riebe, D. E. Granger, J. L. Clayton, J. G. King, and W. F. Megahan (2001), Mountain erosion over 10 yr, 10 k.y., and 10 m.y. time scales, *Geology*, *29*, 591–594.

Klafter, J., and R. Silbey (1980), Electronic-energy transfer in disordered-systems, *J. Chem. Phys.*, *72*(2), 843–848.

Kolmogorov, A. (1951), Solution of a problem in probability theory connected with the problem of the mechanism of stratification, *Trans. Am. Math. Soc.*, *53*, 171–177.

Kuhlemann, J., W. Frisch, I. Dunkl, and B. Szkely (2001), Quantifying tectonic versus erosive denudation by the sediment budget: The Miocene core complexes of the Alps, *Tectonophysics*, *330*, 1–23.

Leopold, L., M. Wolman, and J. Miller (1964), *Fluvial Processes in Geomorphology*, W. H. Freeman, San Francisco, Calif.

Meerschaert, M. M., and H.-P. Scheffler (2004), Limit theorems for continuous-time random walks with infinite mean waiting times, *J. Appl. Probab.*, *41*, 623–638.

Meerschaert, M. M., D. A. Benson, H.-P. Scheffler, and P. Becker-Kern (2002), Governing equations and solutions of anomalous random walk limits, *Phys. Rev. E*, *66*(6), 060102, doi:10.1103/PhysRevE.66.060102.

Meerschaert, M. M., Y. Zhang, and B. Baeumer (2008), Tempered anomalous diffusion in heterogeneous systems, *Geophys. Res. Lett.*, *35*, L17403, doi:10.1029/2008GL034899.

Metzler, R., and J. Klafter (2000), The random walk's guide to anomalous diffusion: A fractional dynamics approach, *Phys. Rep.*, *339*, 1–77.

Molchan, G. M., and D. L. Turcotte (2002), A stochastic model of sedimentation: Probabilities and multifractality, *Eur. J. Appl. Math.*, *13*, 371–383.

Molnar, P. (2004), Late Cenozoic increase in accumulation rates of terrestrial sediment: How might climate change have affected erosion rates?, *Annu. Rev. Earth Planet. Sci.*, *32*, 67–89.

Montroll, E., and M. Schlesinger (1984), Nonequilibrium phenomena II: From stochastic to hydrodynamics, in *Studies in Statistical Mechanics*, vol. 11, edited by J. Lebowitz and E. Montroll, pp. 1–122, North-Holland, Amsterdam.

Montroll, E. W., and G. H. Weiss (1965), Random walks on lattices. II, *J. Math Phys.*, *6*(2), 167–181.

Paola, C., and L. Borgman (1991), Reconstructing random topography from preserved stratification, *Sedimentology*, *38*(4), 553–565.

Paola, C., P. Heller, and C. Angevine (1992), The large scale dynamics of grain size variation in alluvial basins, 1: Theory, *Basin Res.*, *4*, 73–90.

Pelletier, J. D. (2007), Cantor set model of eolian dust deposits on desert alluvial fan terraces, *Geology*, *35*, 439–442.

Pelletier, J. D., and D. L. Turcotte (1997), Synthetic stratigraphy with a stochastic diffusion model of fluvial sedimentation, *J. Sediment. Res.*, *67*(6), 1060–1067.

Plotnick, R. E. (1986), A fractal model for the distribution of stratigraphic hiatuses, *J. Geol.*, *94*(6), 885–890.

Ross, S. (1994), *A First Course in Probability*, 4th ed., Macmillan, Englewood Cliffs, N. J.

Sadler, P. M. (1981), Sediment accumulation rates and the completeness of stratigraphic sections, *J. Geol.*, *89*(5), 569–584.

Sadler, P. (1999), The influence of hiatuses on sediment accumulation rates, in *On the Determination of Sediment Accumulation Rates*, *GeoRes. Forum*, vol. 5, edited by P. Bruns and H. C. Hass, pp. 15–40, Trans Tech., Zurich, Switzerland.

Sadler, P. M., and D. J. Strauss (1990), Estimation of completeness of stratigraphical sections using empirical data and theoretical models, *J. Geol. Soc. London*, *147*, 471–485.

Scher, H., and M. Lax (1973), Stochastic transport in a disordered solid. I. Theory, *Phys. Rev. B*, *7*(10), 4491–4502.

Schmeeckle, M. W., and J. M. Nelson (2003), Direct numerical simulation of bedload transport using a local, dynamic boundary condition, *Sedimentology*, *50*(2), 279–301.

Schumer, R., D. A. Benson, M. M. Meerschaert, and S. W. Wheatcraft (2001), Eulerian derivation for the fractional advection-dispersion equation, *J. Contam. Hydrol.*, *48*, 69–88.

Schumer, R., D. A. Benson, M. M. Meerschaert, and B. Baeumer (2003), Fractal mobile/immobile solute transport, *Water Resour. Res.*, *39*(10), 1296, doi:10.1029/2003WR002141.

Schumer, R., M. M. Meerschaert, and B. Baeumer (2009), Fractional advection-dispersion equations for modeling transport at the Earth surface, *J. Geophys. Res.*, doi:10.1029/2008JF001246, in press.

Singh, A., K. Fienberg, D. J. Jerolmack, J. Marr, and E. Foufoula-Georgiou (2009), Experimental evidence for statistical scaling and intermittency in sediment transport rates, *J. Geophys. Res.*, *114*, F01025, doi:10.1029/2007JF000963.

Strauss, D., and P. M. Sadler (1989), Stochastic models for the completeness of stratigraphic sections, *Math. Geol.*, *21*(1), 37–59.

Sumer, B. M., L. H. C. Chua, N. S. Cheng, and J. Fredsoe (2003), Influence of turbulence on bed load sediment transport, *J. Hydraul. Eng.*, *129*(8), 585–596.

Tipper, J. C. (1983), Rates of sedimentation and stratigraphical completeness, *Nature*, *302*, 696–698.

Zhang, P., P. Molnar, and W. R. Downs (2001), Increased sedimentation rates and grain sizes 2–4 Myr ago due to the influence of climate change on erosion rates, *Nature*, *410*, 891–897.

Zhang, Y., D. A. Benson, and B. Baeumer (2008), Moment analysis for spatiotemporal fractional dispersion, *Water Resour. Res.*, *44*, W04424, doi:10.1029/2007WR006291.

D. J. Jerolmack, Department of Earth and Environmental Science, University of Pennsylvania, Philadelphia, PA 19104, USA. (sediment@sas.upenn.edu)

R. Schumer, Division of Hydrologic Sciences, Desert Research Institute, Reno, NV 89512, USA. (rina@dri.edu)